Electronic Supplementary Information

Experimental section

Materials: Graphite powder (20-80 mesh) was purchased from Alfa Aesar. Potassium permanganate ($KMnO_4$), sulphuric acid (H_2SO_4), hydrochloric acid (HCl), hydrogen peroxide (H_2O_2), ethylene glycol ($C_2H_6O_2$), Iron acetate ($Fe(CH_3COO)_2$), Cobalt acetate ($Co(CH_3COO)_2$), hydrazine hydrate ($N_2H_4.H_2O$), Para-(dimethylamino) benzaldehyde ($C_9H_{11}NO$), Ammonium standard solution (1000 ppm), and sodium nitroferricyanide (III) dihydrate ($Na_2Fe(CN)_5NO{\cdot}2H_2O$) were purchased from Sigma Aldrich Australia. Sodium hypochlorite (NaClO), sodium hydroxide (NaOH), sodium salicylate($C_7H_5O_3Na$), sodium sulfate (Na_2SO_4), and isopropanol (C_3H_8O) were purchased from Chem-supply Australia. Carbon paper (Toray carbon), and Nafion (211) were bought from Fuel cell store. Milli-Q water was used in all experiments.

Preparation of $CoFe_2O_4$/rGO: Graphite oxide (GO) was developed from graphite powder by modified Hummer's method.[1] Synthesized GO was subjected to liquid exfoliation by ultrasonication for 2 h and the non-oxidized layers were separated by centrifugation at 1000 rpm to get graphene oxide dispersed in the ethylene glycol (1 mg mL^{-1}). 20 mL of this dispersion was incorporated with the cobalt acetate (25 mM) and iron acetate (50 mM) at 60 °C for 2h. Later, this solution was transferred to the 45 mL autoclave for solvothermal self-assembly of $CoFe_2O_4$ nanoclusters on graphene at 210 °C for 20h. The resulted product was washed with ethanol, water and dried under vacuum. A similar procedure was used for the synthesis of rGO (without CoFe), Co_3O_4/rGO (without Fe) and Fe_3O_4/rGO (without Co).

Electrode preparation for NRR:

To prepare $CoFe_2O_4$/rGO/CFP, a catalyst ink was prepared by the ultrasonic-assisted dispersion of 10 mg of active material in a mixture of solvent (200 µL H_2O: 750 µL IPA) with Nafion (50

μL) as a binder material. An appropriate amount of catalyst ink was drop cast on a carbon fiber paper (1×1 cm^{-2}) and dried in ambient air to act as a working electrode for NRR evaluations (mass loading of 1 mg cm^{-2}).

Characterizations: Crystalline structure of the material was analyzed by X-ray diffraction (XRD, Malvern Panalytical Empyrean-II X-ray diffractometer) with Co-Kα radiation (λ=1.789 Å). High angle annular dark field (HAADF) – scanning transmission electron microscopy (STEM) images and energy-dispersive X-ray spectroscopy (EDS) mapping were obtained by using JEOL JEM-F200 Multi-Purpose FEG-S/TEM instrument. X-ray photoelectron spectroscopy (XPS) analysis was conducted using the Thermo ESCALAB 250i X-ray photoelectron spectrometer equipped with a monochromatic Al Kα X-ray source (hv =1486.68 eV). UV-vis spectroscopy was carried out on Varian Cary 100 Scan double-beam UV/Vis spectrophotometer. Raman spectra were recorded using a Renishaw inVia 2 Raman spectrometer with a 532 nm laser. Fourier transform infrared spectroscopy (FTIR) was conducted on Thermo Fischer Nicolet iS10 FTIR (IR4). Inductively coupled plasma optical emission spectroscopy (ICP-OES) was conducted on PerkinElmer Optima. Brunauer–Emmett–Teller (BET) surface area was determined by Micromeritics Tristar II Plus 2.02.

Electrochemical NRR evaluation:

The electrochemical measurements were carried out with an electrochemical workstation (CHI 760D) in a H-type double compartment cell. Ag/AgCl and Pt electrodes were used as reference and counter electrodes, respectively. The potentials reported in this work were converted to reversible hydrogen electrode (RHE) scale via calibration with the following equation: E (vs. RHE) = E (vs. Ag/AgCl) + 0.222 V + 0.059 × pH. For electrochemical NRR evaluation, chrono-

amperometry tests were conducted in N_2-saturated 0.1 M Na_2SO_4 solution (electrolyte was purged with N_2 for 30 min before the measurement).

Nafion membrane pretreatment:

The membrane was treated with ultrapure water for 1 h and treated with H_2O_2 (5%) aqueous solution at 80 °C for another 1 h, respectively. And then, the membrane was treated with 0.5 M H_2SO_4 for 3 h at 80 °C and finally in water for 6 h.

Quantification of NH_3:

After chrono-amperometry tests (CA), ammonia quantification was done by Indophenol blue method.[2] In a typical experiment, 2 mL of the electrolyte was collected from cathode chamber and mixed with 2 mL of coloring solution (5 wt% each of salicylic acid and sodium citrate in 1 M NaOH), 1 mL of oxidizing solution (0.05M NaClO), and 0.2 mL of 1 wt% catalyst (Sodium nitroferricyanide) solution, successively. The resulted solution was incubated for 2 h for stable color development and analyzed by UV spectrophotometer at 655 nm. Respective calibration curves were plotted by standard NH_3 solution of different concentrations that shows good linear relation of absorption with NH_3 concentration in three independent calibrations.

Quantification of N_2H_4:

The amount of N_2H_4 produced during this process was estimated by the method of Watt and Chrisp.[3] A mixture of 5.99 g $C_9H_{11}NO$, 30 mL HCl, and 300 mL ethanol was used as a color reagent. A calibration curve was plotted by making standard solutions of N_2H_4 in different concentration. 5 mL of respective concentration was mixed with 5 mL of coloring solution and incubated for 20 min to achieve stable color. The good Linear relation was obtained between N_2H_4 concentration and absorbance in three independent calibration measurements.

Calculation of faradaic efficiency and rate of NH_3 production:

The faradaic efficiency (FE) for N_2 reduction was defined as the amount of electric charge used for synthesizing NH_3 divided the total charge passed through the electrodes during the electrolysis.[4] The total amount of NH_3 produced was measured using colorimetric methods. Assuming three electrons were needed to produce one NH_3 molecule, the FE could be calculated as

$$\text{FE} = \frac{3 \times F \times C_{NH3} \times V}{17 \times Q}$$

The rate of NH_3 formation was calculated as

$$\text{Rate of } NH_3 \text{ formation} = \frac{C_{NH3} \times V}{t \times A}$$

Where F is the Faradays constant, C_{NH3} is the measured ammonia concentration, V is the volume of the electrolyte, A is the geometrical surface area of electrode, t is time for electrolysis and Q is the total charge consumed during electrolysis in coulombs.

Thermodynamic equilibrium potential:

The equilibrium potentials required for NRR in neutral medium can be calculated as follow.

$N_2(gas) + 8H_2O + 6e^- \rightarrow 2NH_4OH\ (aq) + 6OH^-$ $\quad \Delta G^0 = 426.38\ kJ\ mol^{-1}$

$E^0 = -\Delta G^0/nF = -0.737$ V vs SHE (Standard hydrogen electrode)

So, thermodynamic potential in N_2 saturated electrolyte (1 atm) is

$E = E^0 - RT/6F \times \ln [c^2(NH_4OH) \times c^6 (OH^-)] + 0.059 \times pH$

F = Faradays constant (96485 C mol^{-1})

R = Gas constant (8.314 J mol^{-1} K^{-1})

C (OH) = 1.58×10^{-7} M

C (NH_4OH) = 10 μM

pH = 7.2

T = 298.15 K

n (number of electrons) = 6

Thermodynamic equilibrium potential for this reaction is calculated to be -0.196 V vs RHE.

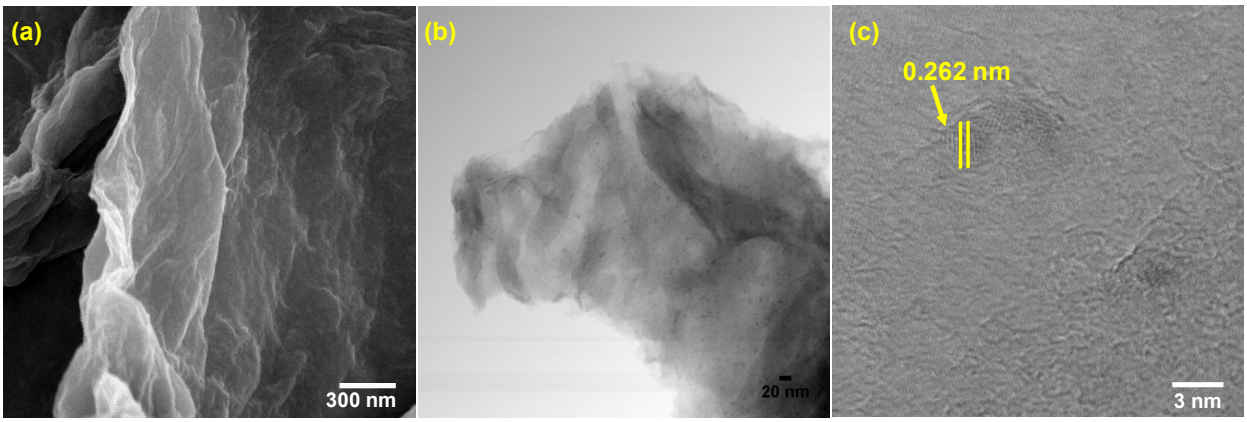

Fig. S1. SEM (a) TEM (b) and HRTEM image of $CoFe_2O_4$/rGO.

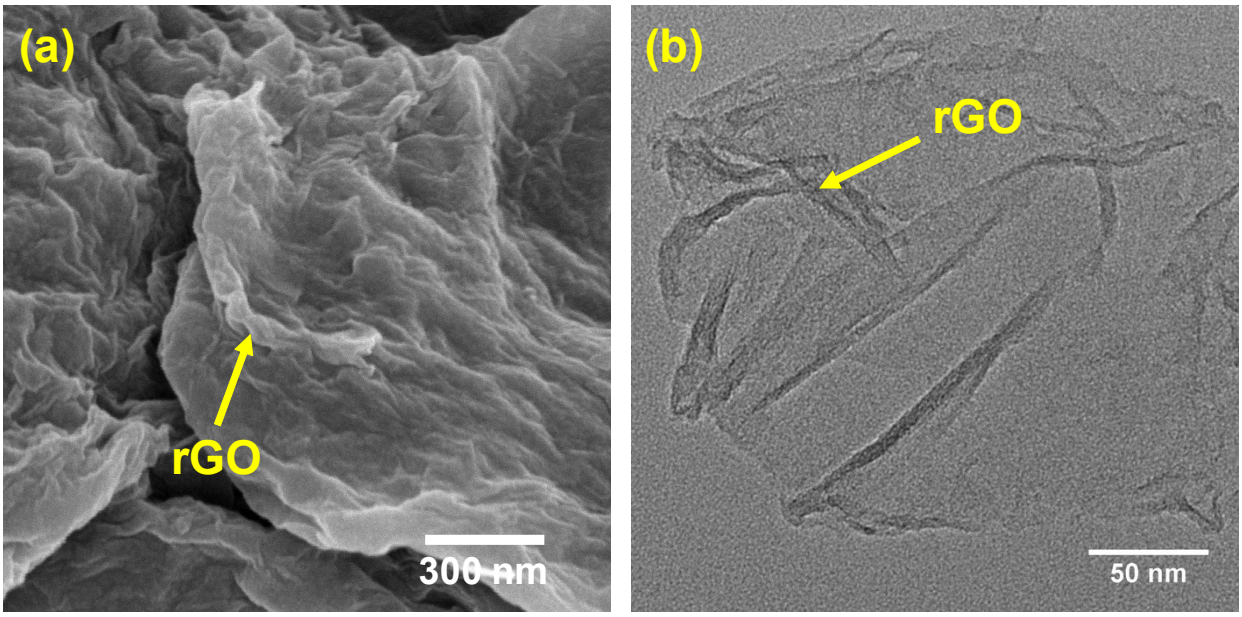

Fig. S2. SEM (a) and TEM (b) image of rGO.

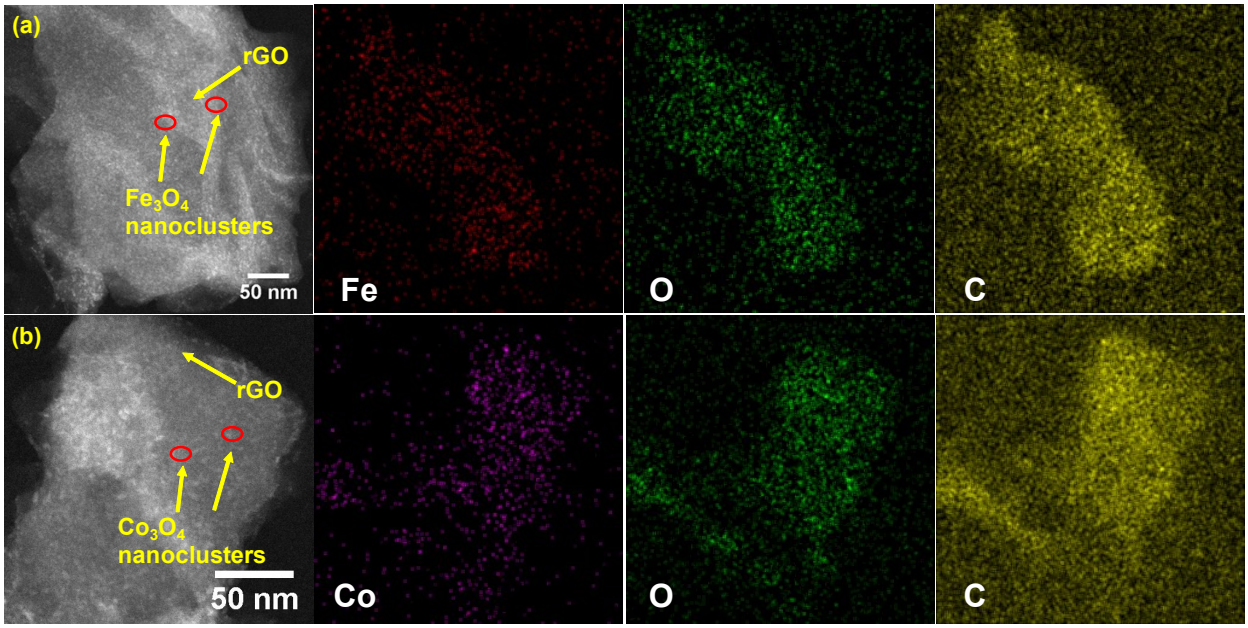

Fig. S3. HAADF-STEM image and STEM-EDS elemental mapping of (a) Fe_3O_4/rGO and (b) Co_3O_4/rGO.

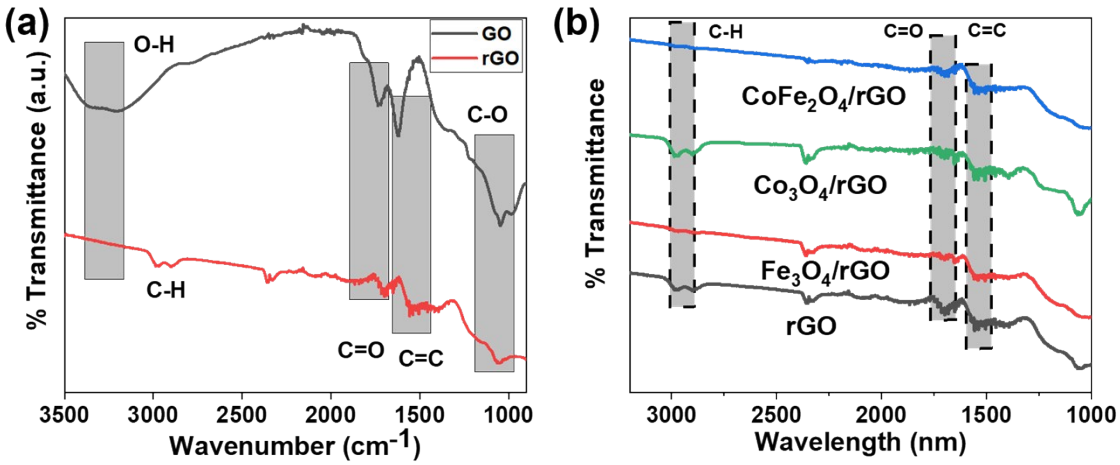

Fig. S4. FTIR spectrum of (a) GO and rGO, and (b) rGO, Fe_3O_4/rGO, Co_3O_4/rGO and $CoFe_2O_4$/rGO.

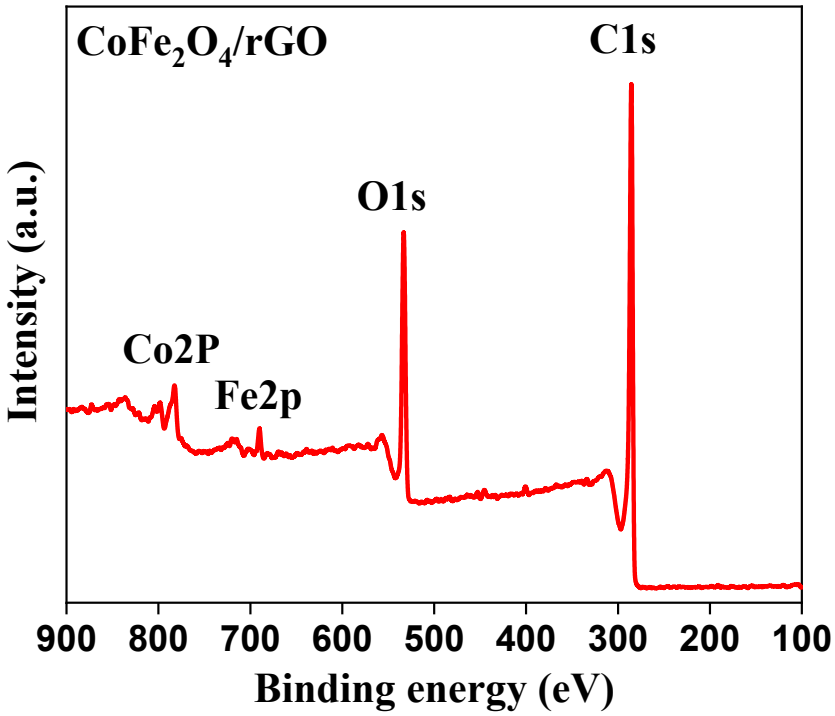

Fig. S5. XPS survey spectrum of $CoFe_2O_4$/rGO.

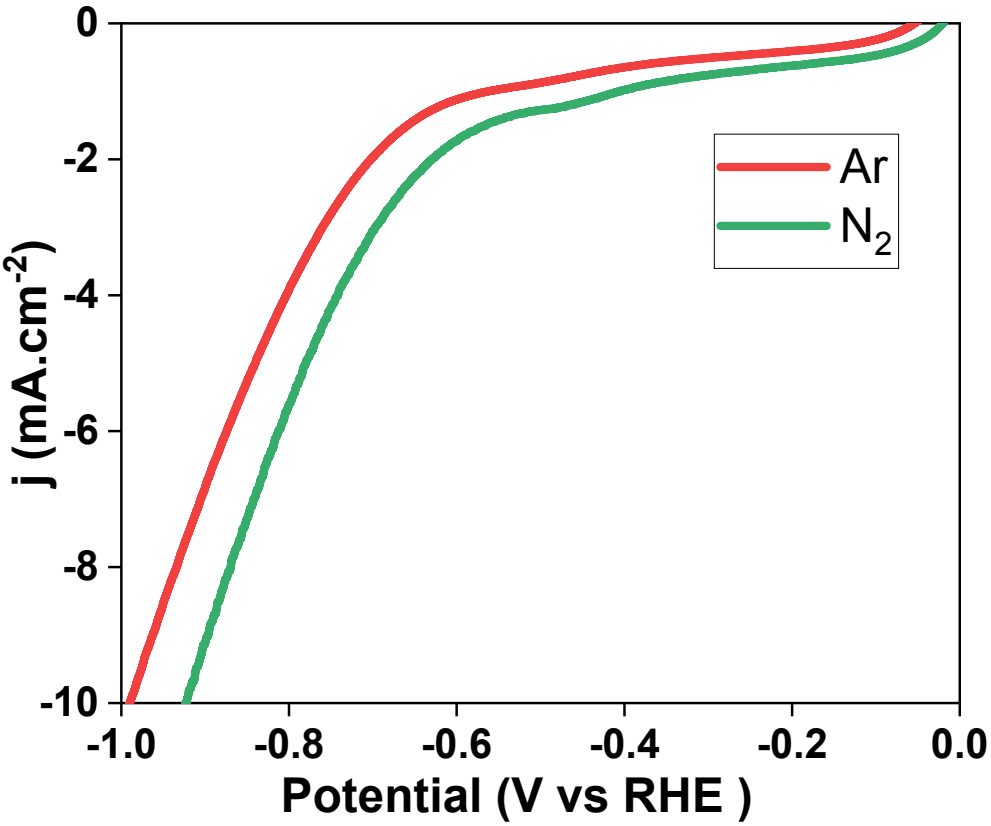

Fig. S6. Linear sweep voltammetry of $CoFe_2O_4$/rGO in Ar and N_2 in 0.1 M Na_2SO_4.

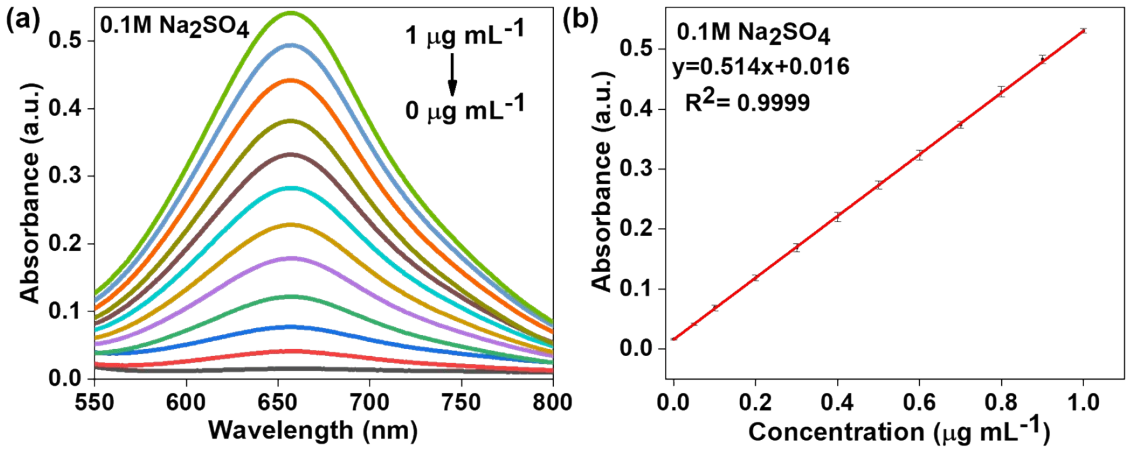

Fig. S7. (a) UV-vis absorption spectra of different NH_3 concentrations stained with indophenol assay for 2h. (b) calibration curve for NH_3 determination.

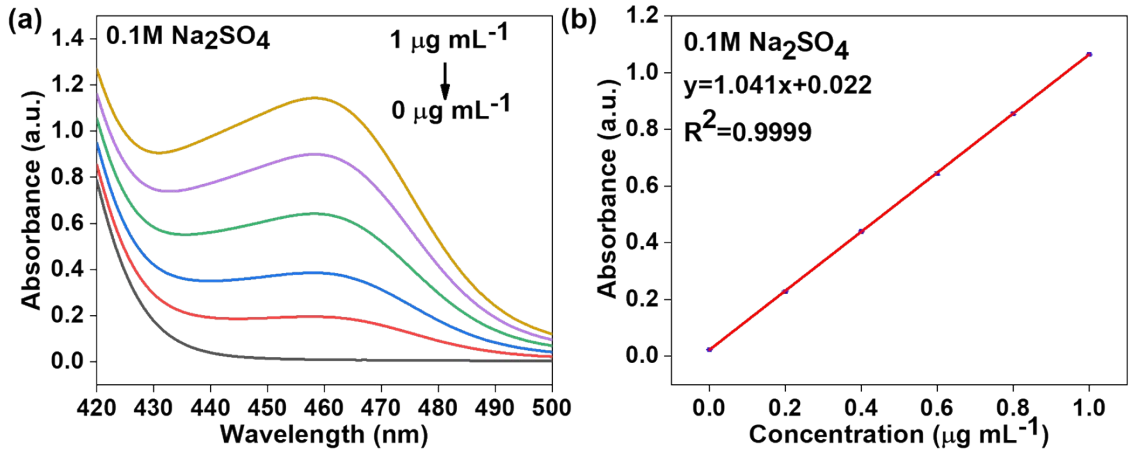

Fig. S8. (a) UV-vis absorption spectra of different N_2H_4 concentration. (b) calibration curve for N_2H_4 determination.

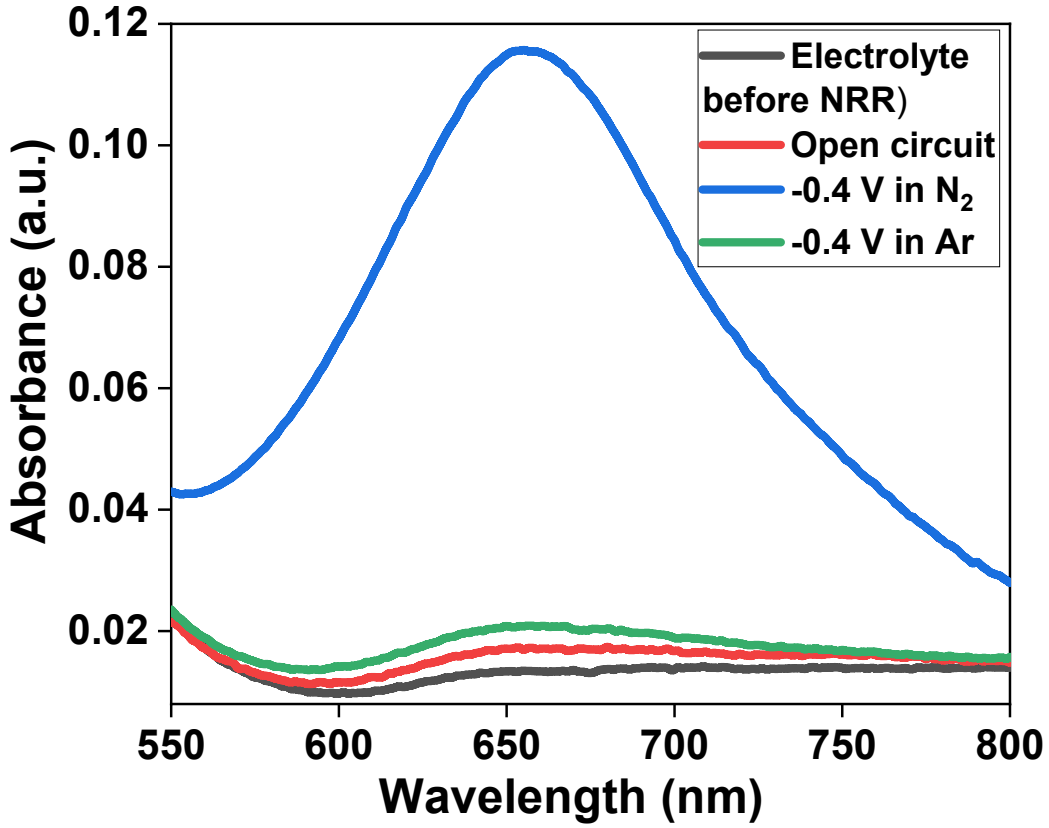

Fig. S9. (a) UV-vis absorption spectra of different control experiments stained by indophenol assay for 2h.

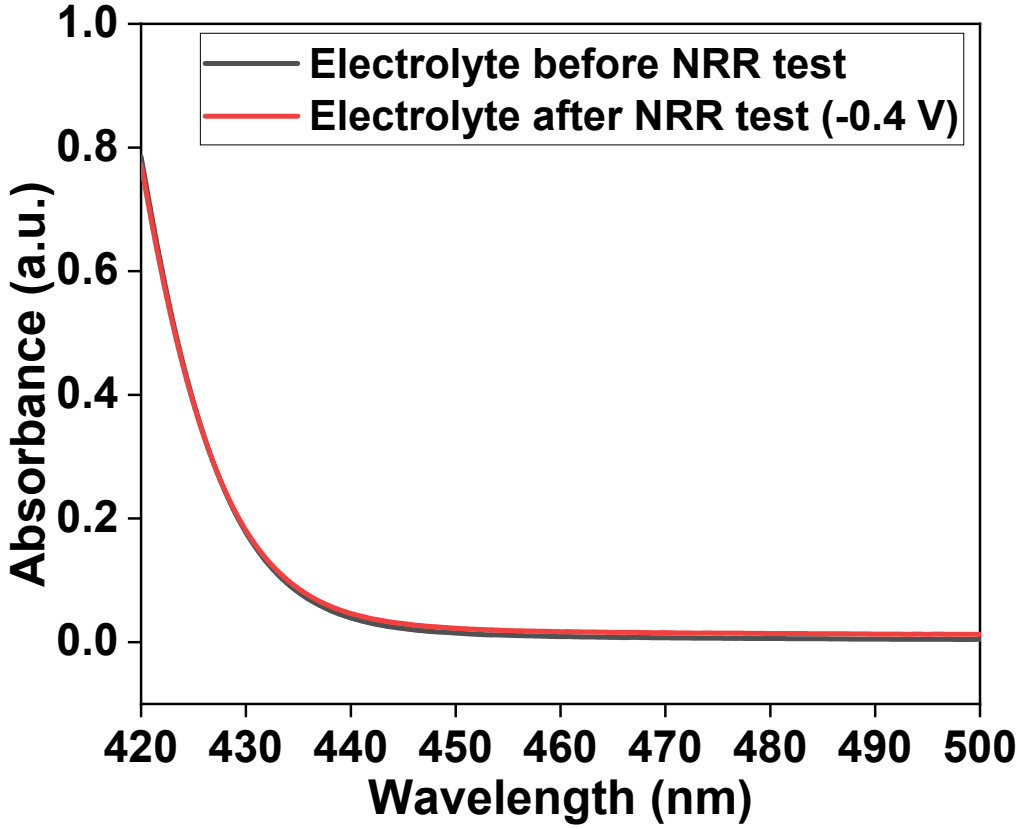

Fig. S10. (a) UV-vis absorption spectra of electrolyte after 2h of electrolysis at -0.4 V for the estimation of N_2H_4 by Watt and Chrisp method.

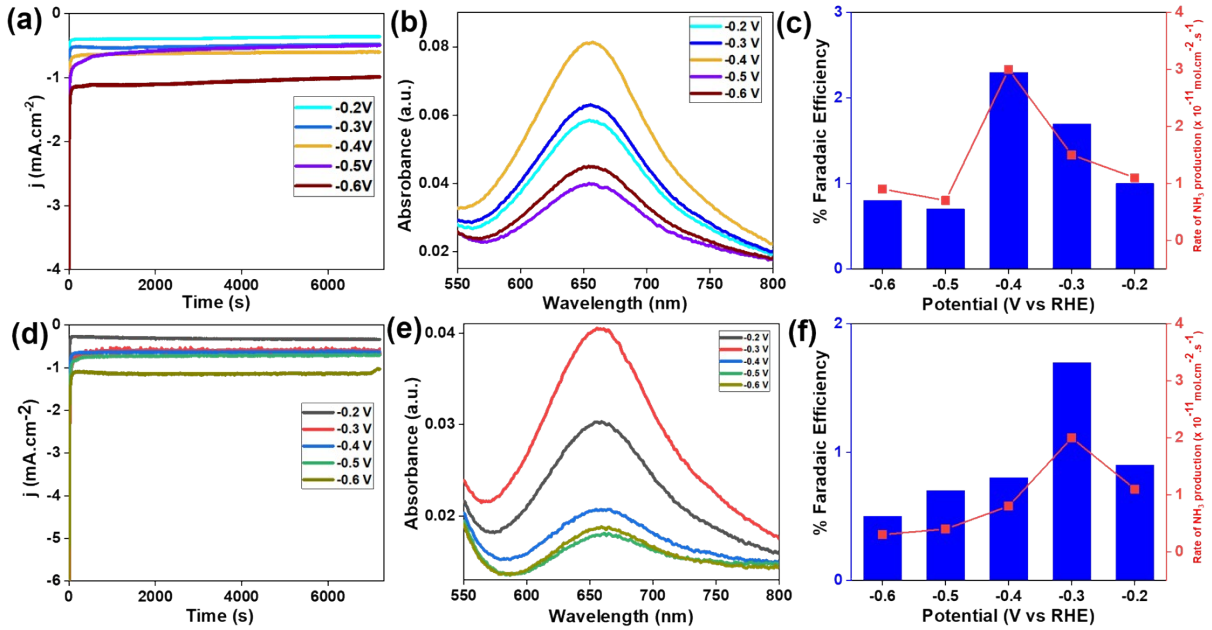

Fig. S11. NRR performance of Fe_3O_4/rGO. (a) Chronoamperometry curves at respective potentials in 0.1 M Na_2SO_4, (b) UV-visible colorimetric spectra at respective potentials stained by indophenol method after 2h electrolysis in N_2, and (c) Corresponding FE and rate of NH_3 production. NRR performance of Co_3O_4/rGO. (d) Chronoamperometry curves at respective potentials in 0.1 M Na_2SO_4, (e) UV-visible colorimetric spectra at respective potentials stained by indophenol method after 2h electrolysis in N_2, and (f) Corresponding FE and rate of NH_3 production.

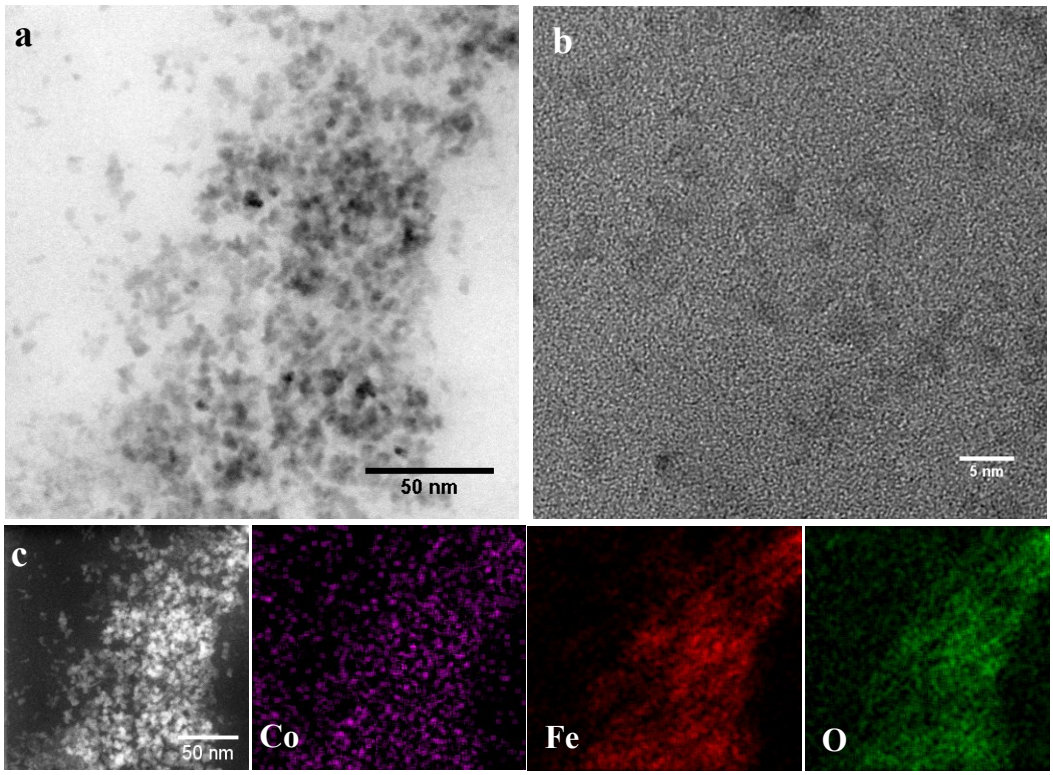

Fig. S12. STEM (a), HRTEM (b), and (c) STEM-EDS mapping of $CoFe_2O_4$/rGO after NRR.

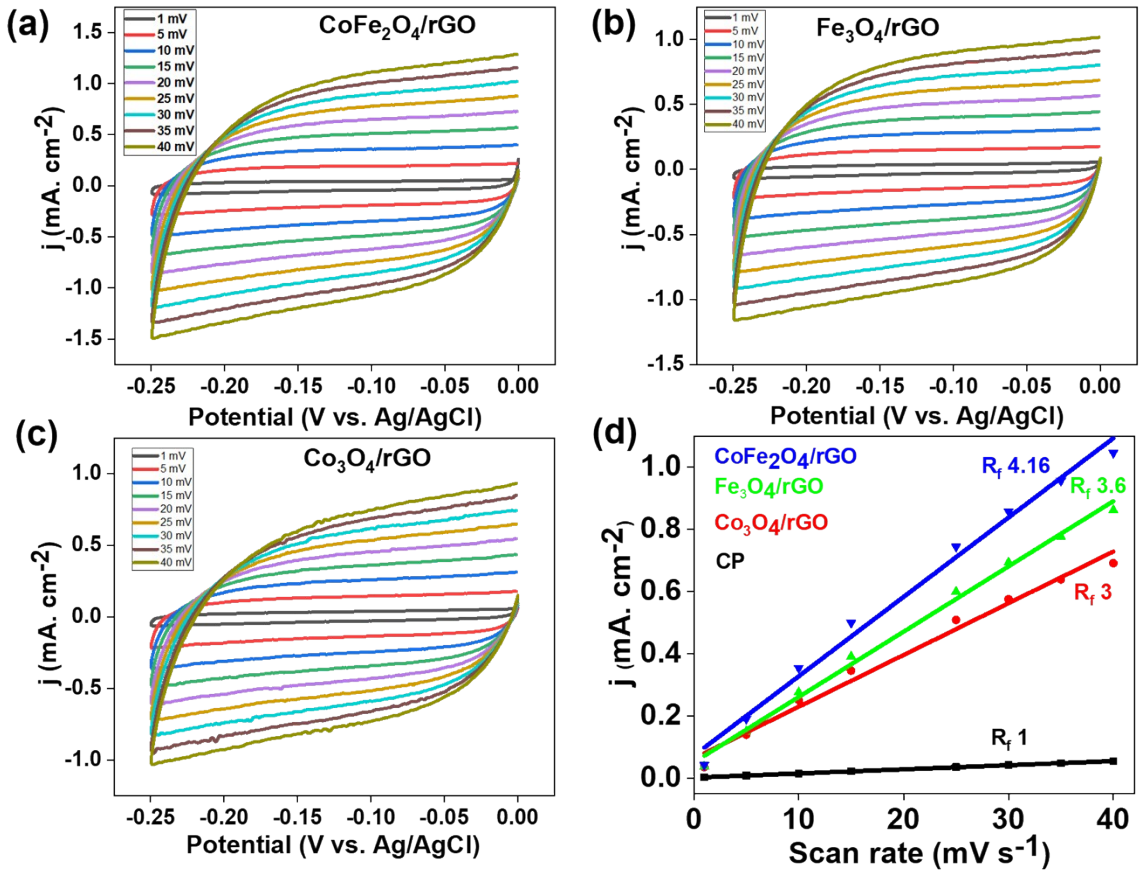

Fig. S13. Double layer capacitance measurements by cyclic voltammetric scan at various scan rate (v) ranging from 1- 40 mV s^{-1} (a) $CoFe_2O_4$/rGO, (b) Fe_3O_4/rGO and (c) Co_3O_4/rGO. Calculated R_f factor for all samples with respect to carbon paper (d).

Table S1: ICP analysis of $CoFe_2O_4$/rGO, Fe_3O_4/rGO and Co_3O_4/rGO.

Sample name	**Co**	**Fe**
	%wt	**%wt**
$CoFe_2O_4$/rGO	1.40	3.30
Co_3O_4/rGO	4.8	0.0
Fe_3O_4/rGO	0.0	4.9

Table S2: BET normalized rate of NH_3 production

Sample name	BET surface area (m^2/g)	BET normalized Rate of NH_3 ($mol\ cm^{-2}\ s^{-1}$)
$CoFe_2O_4$/rGO	133.5	3.14×10^{-13}
Co_3O_4/rGO	140.2	2.13×10^{-13}
Fe_3O_4/rGO	147.8	1.3×10^{-13}
rGO	180.7	2.7×10^{-14}

Table S3: Comparison of NRR performance of CoFe/rGO with other Fe-based electrocatalysts at ambient conditions.

S/No	Catalyst/ Substrate	Electrolyte/ system	Rate of NH_3 production	Faradaic Efficiency (%)	Ref
1	Fe/FTO	Ionic liquids (phosphonium based)	4.7×10^{-12} mol s^{-1} cm^{-2}	60 at -0.8 V vs NHE	[5]
2	α-Fe nanorods@ $Fe3O_4$/CFP	Aprotic solvents-Ionic liquids	2.35×10^{-11} mol s^{-1} cm^{-2}	32 at -0.65 V vs NHE	[6]
3	γ-Fe_2O_3/ CFP	AEM electrolyte	55.96 nmol h^{-1} mg^{-1}	0.044 at 1.6 V_{cell}	[7]
4	Fe/Fe_3O_4	PBS	0.20 μg h^{-1} cm^{-2}	8.29 at -0.3V vs RHE	[8]
5	Spinel Fe_3O_4	0.1 M Na_2SO_4	5.6×10^{-11}mol s^{-1} cm^{-2}	2.6 at -0.4 V vs RHE	[9]
6	β-FeOOH	0.5 M $LiClO_4$	23.32 μg $h^{-1}$$mg^{-1}$	6.7 at -0.70 V vs Ag/AgCl	[10]
7	Fe-N/C	0.1 M KOH	34.83 μg h^{-1} mg_{cat}^{-1}	9.28% at -0.2 V vs RHE	[11]
8	Fe_{SA}-N/C	0.1 M KOH	7.48 μg h^{-1} mg_{cat}^{-1}	56.55% at 0 V vs RHE	[11]
9	$CoFe_2O_4$/r GO	0.1 M Na_2SO_4	4.2×10^{-11} mol s^{-1} cm^{-2}	6.2% at -0.4 V vs RHE	This work

References:

1 D. C. Marcano, D. V. Kosynkin, J. M. Berlin, A. Sinitskii, Z. Sun, A. Slesarev, L. B. Alemany, W. Lu and J. M. Tour, *ACS Nano*, 2010, **4**, 4806–4814.

2 C. Lv, C. Yan, G. Chen, Y. Ding, J. Sun, Y. Zhou and G. Yu, *Angew. Chemie Int. Ed.*, 2018, **57**, 6073–6076.

3 J. Han, Z. Liu, Y. Ma, G. Cui, F. Xie, F. Wang, Y. Wu, S. Gao, Y. Xu and X. Sun, *Nano Energy*, 2018, **52**, 264–270.

4 W. Qiu, X.-Y. Xie, J. Qiu, W.-H. Fang, R. Liang, X. Ren, X. Ji, G. Cui, A. M. Asiri, G. Cui, B. Tang and X. Sun, *Nat. Commun.*, 2018, **9**, 3485.

5 F. Zhou, L. M. Azofra, M. Ali, M. Kar, A. N. Simonov, C. McDonnell-Worth, C. Sun, X. Zhang and D. R. MacFarlane, *Energy Environ. Sci.*, 2017, **10**, 2516–2520.

6 B. H. R. Suryanto, C. S. M. Kang, D. Wang, C. Xiao, F. Zhou, L. M. Azofra, L. Cavallo, X. Zhang and D. R. MacFarlane, *ACS Energy Lett.*, 2018, **3**, 1219–1224.

7 J. Kong, A. Lim, C. Yoon, J. H. Jang, H. C. Ham, J. Han, S. Nam, D. Kim, Y. Sung, J. Choi and H. S. Park, *ACS Sustain. Chem. Eng.*, 2017, **5**, 10986–10995.

8 L. Hu, A. Khaniya, J. Wang, G. Chen, W. E. Kaden and X. Feng, *ACS Catal.*, 2018, **8**, 9312–9319.

9 Q. Liu, X. Zhang, B. Zhang, Y. Luo, G. Cui, F. Xie and X. Sun, *Nanoscale*, 2018, **10**, 14386–14389.

10 X. Zhu, Z. Liu, Q. Liu, Y. Luo, X. Shi, A. M. Asiri, Y. Wu and X. Sun, *Chem. Commun.*,

2018, **54**, 11332–11335.

11 M. Wang, S. Liu, T. Qian, J. Liu, J. Zhou, H. Ji, J. Xiong, J. Zhong and C. Yan, *Nat. Commun.*, 2019, **10**, 341.